

# Accepted Manuscript

Optical and electrochemical behavior of new nano-sized complexes based on gold-colloid and Co-porphyrin derivative in the presence of H<sub>2</sub>O<sub>2</sub>

Eugenia Fagadar-Cosma, Iuliana Sebarchievici, Anca Lascu, Ionela Creanga, Anca Palade, Mihaela Birdeanu, Bogdan Taranu, Gheorghe Fagadar-Cosma

PII: S0925-8388(16)31969-7

DOI: [10.1016/j.jallcom.2016.06.246](https://doi.org/10.1016/j.jallcom.2016.06.246)

Reference: JALCOM 38115

To appear in: *Journal of Alloys and Compounds*

Received Date: 7 April 2016

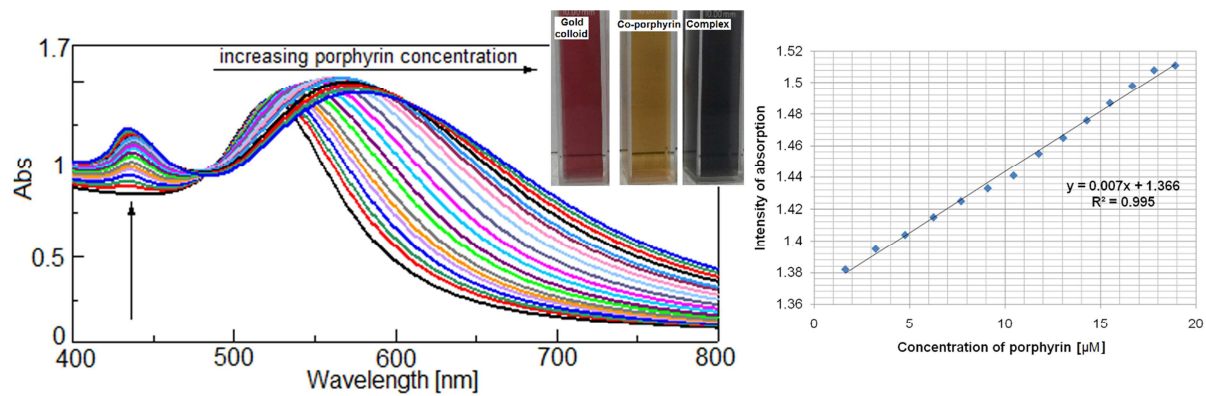
Revised Date: 26 May 2016

Accepted Date: 24 June 2016

Please cite this article as: E. Fagadar-Cosma, I. Sebarchievici, A. Lascu, I. Creanga, A. Palade, M. Birdeanu, B. Taranu, G. Fagadar-Cosma, Optical and electrochemical behavior of new nano-sized complexes based on gold-colloid and Co-porphyrin derivative in the presence of H<sub>2</sub>O<sub>2</sub>, *Journal of Alloys and Compounds* (2016), doi: [10.1016/j.jallcom.2016.06.246](https://doi.org/10.1016/j.jallcom.2016.06.246).

This is a PDF file of an unedited manuscript that has been accepted for publication. As a service to our customers we are providing this early version of the manuscript. The manuscript will undergo copyediting, typesetting, and review of the resulting proof before it is published in its final form. Please note that during the production process errors may be discovered which could affect the content, and all legal disclaimers that apply to the journal pertain.





ACCEPTED MANUSCRIPT

**OPTICAL AND ELECTROCHEMICAL BEHAVIOR OF NEW NANO-SIZED  
COMPLEXES BASED ON GOLD-COLLOID AND Co-PORPHYRIN DERIVATIVE IN  
THE PRESENCE OF H<sub>2</sub>O<sub>2</sub>**

**Eugenia FAGADAR-COSMA<sup>a\*</sup>, Iuliana SEBARCHIEVICI<sup>b</sup>, Anca LASCU<sup>a</sup>, Ionela  
CREANGA<sup>a</sup>, Anca PALADE<sup>a</sup>, Mihaela BIRDEANU<sup>a,b</sup>, Bogdan TARANU<sup>b</sup>,  
Gheorghe FAGADAR-COSMA<sup>c</sup>**

<sup>a</sup> *Institute of Chemistry Timisoara of Romanian Academy, M. Viteazul Ave. 24, 300223-Timisoara, Romania, [efagadar@yahoo.com](mailto:efagadar@yahoo.com), Tel: +40256/491818; Fax: +40256/491824*

<sup>b</sup> *National Institute for Research and Development in Electrochemistry and Condensed Matter, 1 Plautius Andronescu Street, 300569 Timisoara, Romania*

<sup>c</sup> *Politehnica University of Timisoara, Vasile Parvan Street 6, 300223-Timisoara, Romania,*

**Abstract**

A wide band absorption hybrid material, prepared from a metalloporphyrin and gold nanoparticles (**nAu**) with the purpose to develop optical and electrochemical detection of hydrogen peroxide was investigated.

Gold nanoparticles smaller than 20 nm were obtained and functionalized with Co(II) 5,10,15,20-meso-tetra(3-hydroxyphenyl)porphyrin (**Co-3OHPP**). The dependence between the intensity of absorption of the gold plasmonic band and the increasing concentration of **Co-3OHPP** proved that **nAu** is sensitive to porphyrin detection, showing potential in early medical diagnosis.

The **nAu**-porphyrin complex was exposed to increased amounts of  $\text{H}_2\text{O}_2$  to prove its sensing capacity and the changes of the absorption spectra were monitored by UV-vis spectroscopy. The AFM and FT-IR studies showed significant structural and morphological modifications of the hybrid material after  $\text{H}_2\text{O}_2$  exposure.

In order to verify if the range of physiologically-relevant  $\text{H}_2\text{O}_2$  concentration levels (5–35  $\mu\text{M}$ ) might be detected, three modified glassy carbon (**GC**) electrodes were realized, by deposition onto their surfaces of **nAu** and Co-porphyrin (alone and in successive layers) and were tested to evidence the electrochemical response for  $\text{H}_2\text{O}_2$ . The comparative linear and cyclic voltammetry of the bare and modified **GC** electrodes evidenced an increased electrocatalytic effect on the reduction of  $\text{H}_2\text{O}_2$  onto **GC** electrode modified with **nAu/ Co-3OHPP** ordered layers.

**Keywords:** Co-porphyrin, gold colloid, UV-vis spectroscopy, modified GC-electrodes, voltammetry, electrocatalysis.

## 1. Introduction

The capacity of metalloporphyrins to produce, detect, transport and even store gases and to undergo facile reduction and oxidation is known since the discovery of hemoglobin and chlorophyll [1]. Obtaining of porphyrin based hybrid systems that are capable to preserve the porphyrin amazing optical and catalytic properties [2] by incorporation into a matrix, organic or inorganic, in order to develop new multifunctional materials, represents the actual approach in research. Among the metalloporphyrins, Co(II)-porphyrins are active in catalytic aziridination of styrene [3] and possess electrocatalytic properties for transformation of  $\text{H}_2\text{O}$  into  $\text{H}_2$  and  $\text{O}_2$ ,

respectively [4]. Besides, cobalt-porphyrin based organic matrices have been reported as new kind of electrocatalysts for oxygen reduction reaction [5]. Moreover, the mechanism for molecular oxygen reduction, in basic environment, was established to undergo via a two-electron process to  $H_2O_2$  or by a direct four-electron reaction. The most important finding is that the cobalt catalytic centre in the porphyrin moiety preserves its electrocatalytic property even after the self-assembling process took place [6].

Another complex between Co(II) porphyrin and lipoic acid, deposited on gold electrodes, exhibited catalytic activity towards the reduction of molecular oxygen, this time in acidic solution [7]. The same catalytic performance for oxygen reduction in high acidic media, at room temperature, was obtained by grafting a Co(II) porphyrin onto multiwalled carbon nanotubes [8] and onto the network of three-dimensionally distributed gold (polyoxometallate-modified) nanoparticles producing cobalt porphyrin-hybrid multi-layered film with high activity toward electroreduction of hydrogen peroxide [9]. Electroactive hybrid films of gold colloid nanoparticles and cobalt porphyrins fabricated with layer-by-layer assembly method showed catalytic activity toward the oxygen reduction. The catalytic activity decreases when bilayer number increases due to aggregation of the [AuNP/cobalt porphyrin] hybrid [10].

Spintronic molecular device applications were started after the demonstration that spin states of Co-porphyrin on Au(III) can be reversibly switched over by binding and unbinding of the nitrogen oxide (NO) molecule. After NO exposure, a molecular complex NO-Co-porphyrin was generated [11]. The Kondo effect explained this switching phenomenon by scattering of conduction electrons in cobalt due to magnetic impurities and as a consequence changing of electrical resistivity function of temperature.

Metal nanosized particles are of constant interest due to their controllable surface-to-volume ratio and their hybrids with porphyrins have properties that can be adjusted depending on the obtaining method [12]. For example, 5,10,15,20-tetraphenyl-21H,23H-porphine cobalt-platinum-functionalized reduced graphene oxide was used for sensitive electrochemical detection of Aflatoxin [13].

Porphyrins modified gold nanoparticles of 5-20 nm have low cytotoxicity, fair fluorescence emission and reliable cell uptake ability [14]. Gold nanoparticles of this size are ideal carriers to deliver the porphyrin molecules into cells, thus providing an improved agent in PDT and molecular imaging. Gold nanoparticles of 1–2 nm in diameter could be more toxic due to the possibility of irreversible binding to the biopolymers in cells [15]. Functionalization of gold nanoparticles with organic moieties containing nitrogen represents a source of successful materials for sensor formulations. In this respect, N-methylimidazole-functionalized gold nanoparticles were reported to recognize bis- and tris-Zn-porphyrins [16].

Encouraged by our previous results in H<sub>2</sub>O<sub>2</sub> and CO<sub>2</sub> detection using porphyrins in combination with various inorganic/polymeric matrices [17, 18], the next step of this research was to create a new sensitive material, that can optically or electrochemically detect minute quantities of H<sub>2</sub>O<sub>2</sub> (in the range of 5–35 μM, representing relevant levels in human physiology) and which might easily be incorporated in a detection device. Gold nanoparticles smaller than 20 nm in which total extinction is nearly all contributed by absorption [19] have been functionalized with Co(II) 5,10,15,20-*meso*-tetra(3-hydroxyphenyl) porphyrin (Fig. 1) in order to achieve a better nanomaterial for H<sub>2</sub>O<sub>2</sub> monitoring.

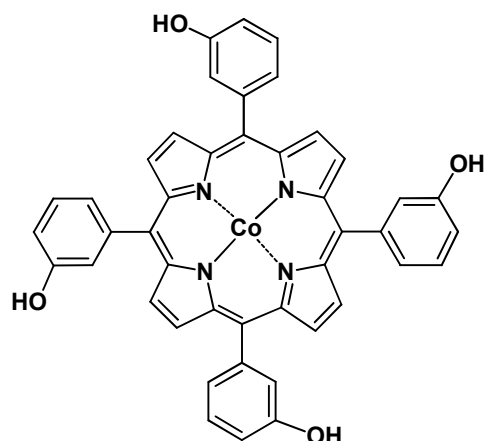


**Fig. 1.** Structure of Co(II) 5,10,15,20-*meso*-tetra(3-hydroxyphenyl) porphyrin  
(**Co-3OHPP**)

In order to extend the possibility of application of the **nAu/ Co-3OHPP** complex, three modified glassy carbon (**GC**) electrodes were realized by deposition onto their surfaces of **nAu** and **Co-3OHPP** alone and of ordered layers (**nAu- Co-3OHPP**) and were comparatively tested by linear and cyclic voltammetry to evidence the best electrochemical response for  $\text{H}_2\text{O}_2$ .

## 2. Experimental

### 2.1. Apparatus

A JASCO UV-visible spectrometer, model V-650, was used for recording UV-visible spectra in various solvents (THF, THF-aqueous system) using quartz cuvettes of 1 cm length. A Nanosurf<sup>®</sup> Easy Scan 2 Advanced Research AFM was used for AFM imaging, carried out in ambient conditions. The samples were obtained by drop casting on silica plates. FT-IR spectra were carried out in ATR mode, in the  $4000\text{-}400\text{ cm}^{-1}$  range on a JASCO 430 apparatus. TEM and STEM analysis of the samples was performed using a Titan G2 80-200 TEM/STEM microscope (FEI Company, the Netherlands) operating at 80kV (image from Fig. 3) 200 kV (image from Fig.

6). Samples for TEM analysis were prepared on carbon-coated copper grids by placing 2  $\mu\text{L}$  of diluted (1:3 v/v) solution of gold colloid. The water was evaporated under vacuum. In order to study the interaction between **Co-3OHPP** and **nAu**, the porphyrin was dissolved in THF and the resulting solution (0.15 mM) was drop-casted together with the nAu solution (diluted 1:4 with double-distilled water) on 200 mesh copper grids covered with carbon film.

Electrochemical measurements were performed on a VoltaLab PGZ 301 potentiostat (Radiometer Analytical). A conventional three-electrode system was used for linear/cyclic voltammetry studies. A platinum wire was used as auxiliary electrode, saturated calomel electrode (SCE) as reference electrode and glassy carbon (**GC**, 0.07  $\text{cm}^2$ ) modified with the synthesized **Co-3OHPP** and gold nanoparticles (**nAu**) as working electrodes. All potentials were measured with respect to the SCE electrode. The electrocatalysis of hydrogen peroxide reduction was carried out in 0.05 M phosphate buffer solution (PBS)/0.05M KCl, pH 5.8, at a scan rate of 50  $\text{mVs}^{-1}$ . All the experiments were carried out at room temperature and the cell was open to the atmosphere. The parameters for the square wave voltammetry (SWV) were: step potential 50 mV; amplitude 5 mV and duration 0.1 sec, scan rate 50 mV/s.

## 2.2. Materials

All reagents were acquired of highest purity from Merck and Fluka and used without further purification. Doubly distilled water was used for the solutions. Buffer solutions (0.05M KCl, pH=5.8) were prepared from  $\text{NaH}_2\text{PO}_4$ ,  $\text{Na}_2\text{HPO}_4$  and  $\text{H}_3\text{PO}_4$ . The porphyrin base, 5,10,15,20-*meso*-tetra(3-hydroxyphenyl) porphyrin, was obtained by Adler method, according to [20].

2.2.1. *Synthesis of Co(II) 5,10,15,20-meso-tetra(3-hydroxyphenyl) porphyrin (Co-3OHPP)*. The synthesis was done by adapting the previous reported method [21]. A solution of 0.2 g ( $0.29 \times 10^{-4}$

<sup>3</sup> mole) 5,10,15,20-meso-tetra(3-hydroxyphenyl) porphyrin in 60 mL THF is brought to reflux under intense stirring in a round bottom three necked flask equipped with magnetic stirrer and refrigerator. Another solution comprised of 0.72 g ( $3.02 \times 10^{-3}$  mole)  $\text{CoCl}_2 \times 6\text{H}_2\text{O}$  dissolved in 40 mL  $\text{CH}_3\text{OH}$  is heated and then dropwise added to the porphyrin solution (final molar ratio porphyrin: metal salt = 1:10). The reaction is monitored by registering the UV-vis spectra every 10 minutes (Fig. 2). The refluxing and stirring of the mixture are maintained for 45 minutes. The solvent mixture is evaporated then the dry product is repeatedly washed with distilled water until the water is clear and all the excess cobalt salt is removed. The product is then dried and recrystallized from  $\text{CHCl}_3$ .

*2.2.2. Synthesis of gold nanoparticles.* The modified method of synthesis belongs to sustainable chemistry [22]. An amount of 0.035 g  $\text{HAuCl}_4 \times 3\text{H}_2\text{O}$  ( $0.088 \times 10^{-3}$  mole) is solved in 116.2 mL doubly distilled water and brought to reflux in a 150 mL three necked flask equipped with magnetic stirrer and refrigerator. Then 12.25 mL (1 wt %) solution of trisodium citrate (0.122 g,  $0.41 \times 10^{-3}$  mole) in doubly distilled water is added at once and the mixture is vigorously stirred and refluxed for 15 minutes. The molar ratio gold salt:sodium citrate = 1:5. The solution turns from yellow to black and then to dark red.

*2.2.3. The complex Co-3OHPP-nAu formation.* The experiment was conducted as follows: gold colloid solution, 3 mL ( $0.47 \times 10^{-3}$  M) was treated with portions of 50  $\mu\text{L}$  Co-3OHPP solution in THF ( $10^{-5}$  M). The mixture was stirred and then the UV-vis spectrum was recorded for each step.

*2.2.4. Preparation of nAu/Co-3OHPP composite modified electrodes.* Prior to each experiment the glassy carbon (GC) surface was mechanically polished to a mirror using fine grade emery papers (5 and 0.3  $\mu\text{m}$ ), then washed ultrasonically in bi-distilled water and acetone for three minutes respectively. After that, the electrode was electrochemically cleaned in sulfuric acid

solution (0.5 M) and the surface was again washed with bi-distilled water and ethanol and allowed to dry.

The **nAu** film was formed by drop-casting (5  $\mu\text{L}$ ) of the colloidal solution (0.68 mM), onto the well cleaned **GC** surface and left to dry, followed by rinsing with water. The Coporphyrin film was formed by drop-casting (3  $\mu\text{L}$ ) from 1.1 mM methanol solution onto the **GC** surface, or **GC/nAu** surface and left to dry. Then the surface was rinsed with methanol and water and left to dry in the dark.

### 3. Results and discussion

The continuous monitoring of the UV-vis changes during the obtaining of **Co-3OHPP** by the metalation reaction put into evidence a significant red shifting of the Soret band with 9 nm in comparison to the porphyrin base (Fig. 2, line 1), accompanied by the decrease in intensity of absorption. Regarding the Q bands, a change in shape can be observed along with a lesser resolution and their number is reduced (Fig. 2, lines 2-6). After purification, the **Co-3OHPP** metalloporphyrin absorption bands are large and increased in intensity (Fig. 2, line 7) in comparison with the porphyrin base, at the same concentration. The Soret band is broadened and red shifted from 418 nm in bare porphyrin to 427 nm in **Co-3OHPP** metalloporphyrin and accompanied by a single well defined Q band located at 543 nm.

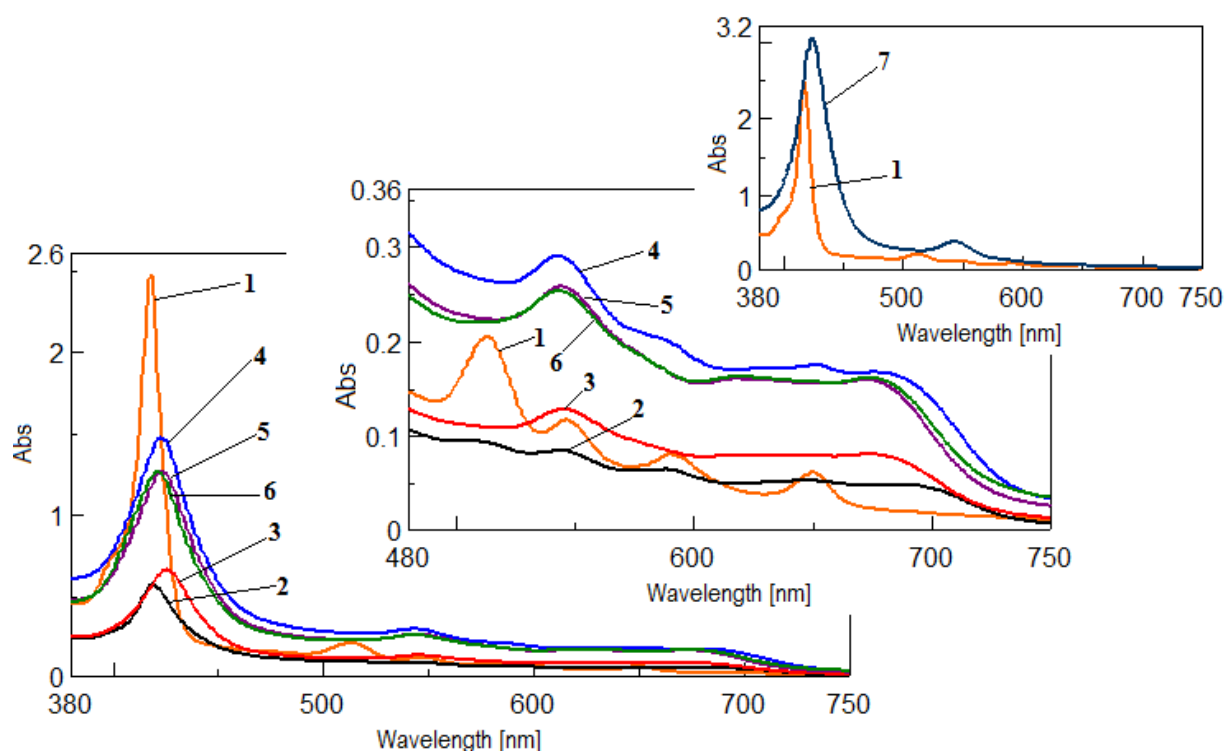


**Fig. 2.** UV-vis monitoring of **Co-3OHPP** synthesis: porphyrin base (line 1) and reaction mixture after: 5 minutes reflux (line 2): 15 minutes reflux (line 3): 25 minutes reflux (line 4); 35 minutes reflux (line 5); 45 minutes reflux (line 6) and the **Co-3OHPP** recrystallized product (line 7)

The presence of only one Q band in the metalloporphyrin absorption spectrum confirms the increase in symmetry due to the metal insertion into the porphyrin core.

The UV-vis spectrum of the gold colloid displays a plasmonic band located at 522 nm and spherical/ovoid shaped nonaggregated particles having diameters in the range 15-20 nm (Fig. 3).

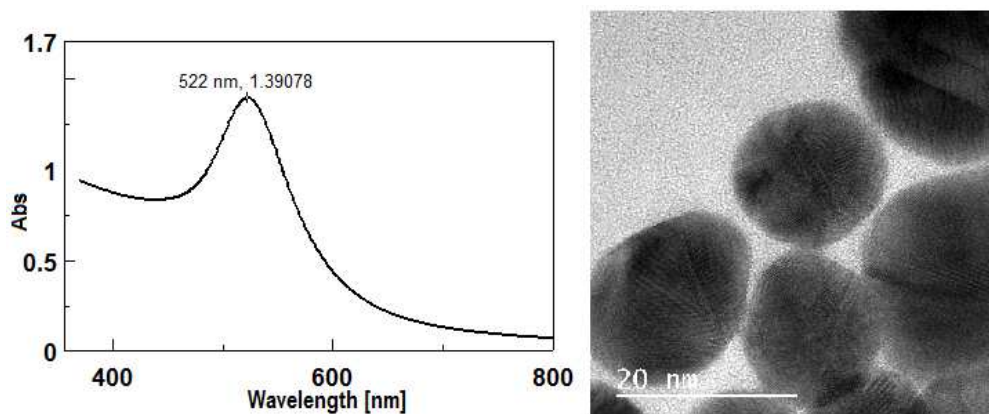


**Fig. 3.** UV-vis spectrum and TEM image of the gold colloid solution ( $c=0.47\times 10^{-3}$  mole/L)

The obtaining of **Co-3OHPP-nAu** hybrid was realized by adding of small amounts of **Co-3OHPP** compound into the gold colloid solution and was continuously monitored by UV-vis spectroscopy (Fig. 4). An isosbestic point located at 484 nm proved the complex formation between the Co-porphyrin and the colloidal gold. The complex generation and some expected aggregation phenomena are sustained by the significant broadening and shifting of the gold plasmonic band from 522 nm up to 600 nm. All these changes occur with noticeable increases in absorption intensity. These types of nanomaterials, with wide band absorption covering all visible spectrum, are considered to have great potential as multifunctional hybrid materials with applications as photosensitizers both in PDT and in formulation of photovoltaic cells. Another isosbestic point (located at 610 nm) helps us to determine the stability of the **Co-3OHPP-nAu** complex that suffers consecutive changes after a certain concentration in porphyrin is reached. This second isosbestic point is associated with the decrease of the plasmon absorption capacity so that we can conclude that the first complex is stable in the range of 1-19  $\mu\text{M}$  porphyrin concentration.

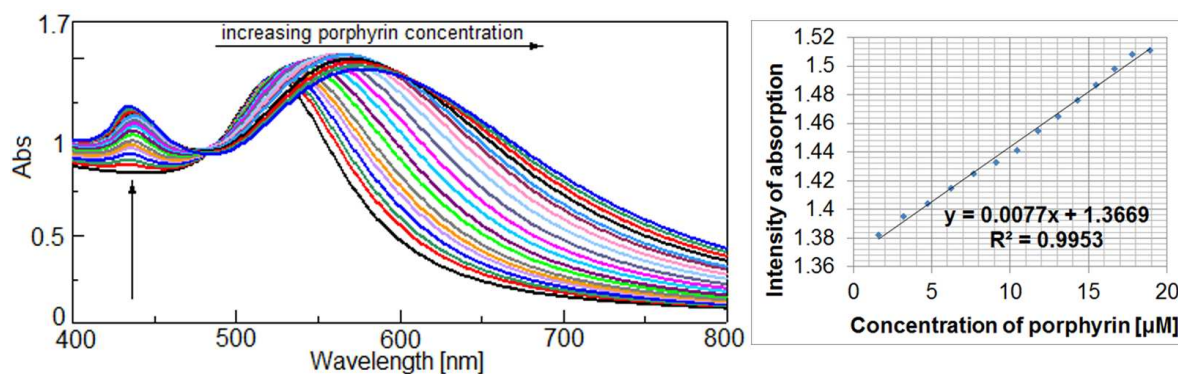


**Fig. 4.** UV-vis spectra recorded by adding **Co-3OHPP** to the gold colloid solution. The dependence between the concentration of **Co-3OHPP** and the intensity of the plasmon absorption.

With increasing the concentration of Co-porphyrin, the Soret band of the **Co-3OHPP-nAu** hybrid suffers a hyperchromic effect. Besides, the absorption band of the gold plasmon increases in intensity in an almost perfect linear fashion (Fig. 4) with increasing the amounts of Co(II)-porphyrin, meaning that gold colloid is suitable as optical sensor for small amounts of porphyrin detection. This result might find valuable medical applications due to the importance in detecting porphyrin derivatives and metabolites present in the human body in early diagnosis of different diseases [23].

The generation of the complex between the Co-porphyrin and the colloidal gold is also accompanied by changes in color. An unexpected violet-blue color of the complex was obtained from the starting materials that are colored in red and respectively yellow (Fig. 5) and that was proven by TEM images to be given by newly formed complex aggregates (Fig. 6).



**Fig. 5.** Color change of solutions during the formation of the **Co-3OHPP-nAu** complex. Red gold colloid (1); yellow **Co-3OHPP** (2); violet-blue gold-porphyrin complex (3).

The dendritic structure observed in Fig. 6a is comprised mainly of **Co-3OHPP** H- and J-type self-aggregates due to their interaction with gold nanoparticles. The disk shaped structures from Fig. 6c can be attributed to the metalloporphyrin associated by sandwich type process, that was previously reported in our papers [24, 25].

On the other hand, the gold nanoparticles are associated in chains of 3-4 round particles and in higher disordered associations as can be seen in Figs. 6b and 6d.

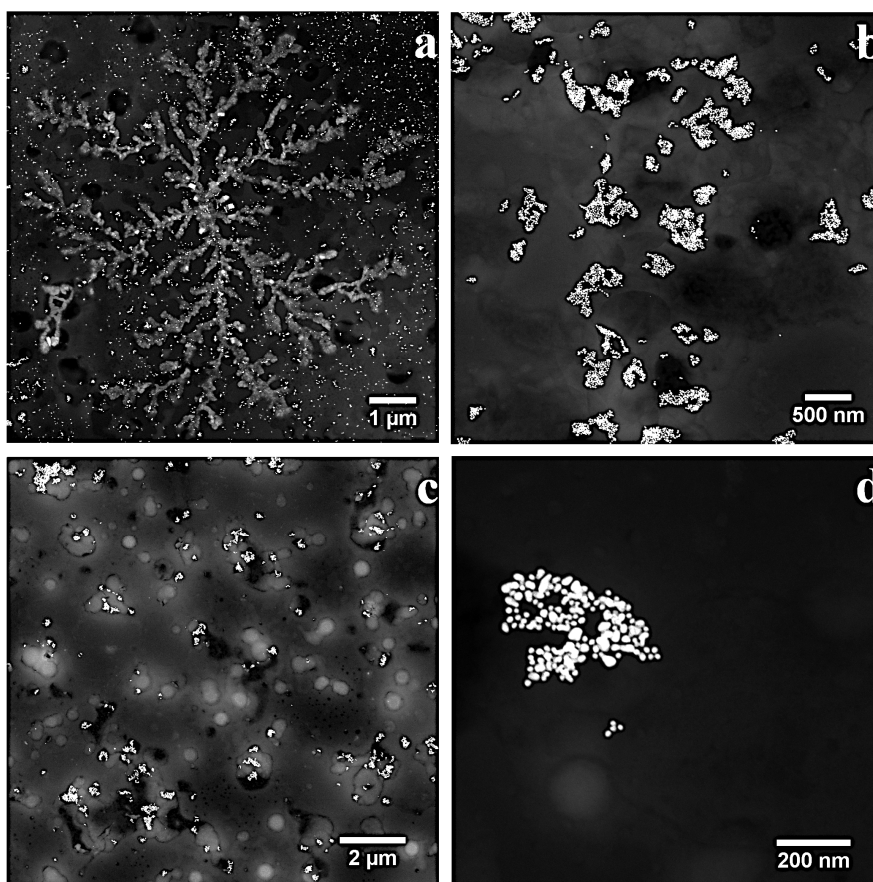
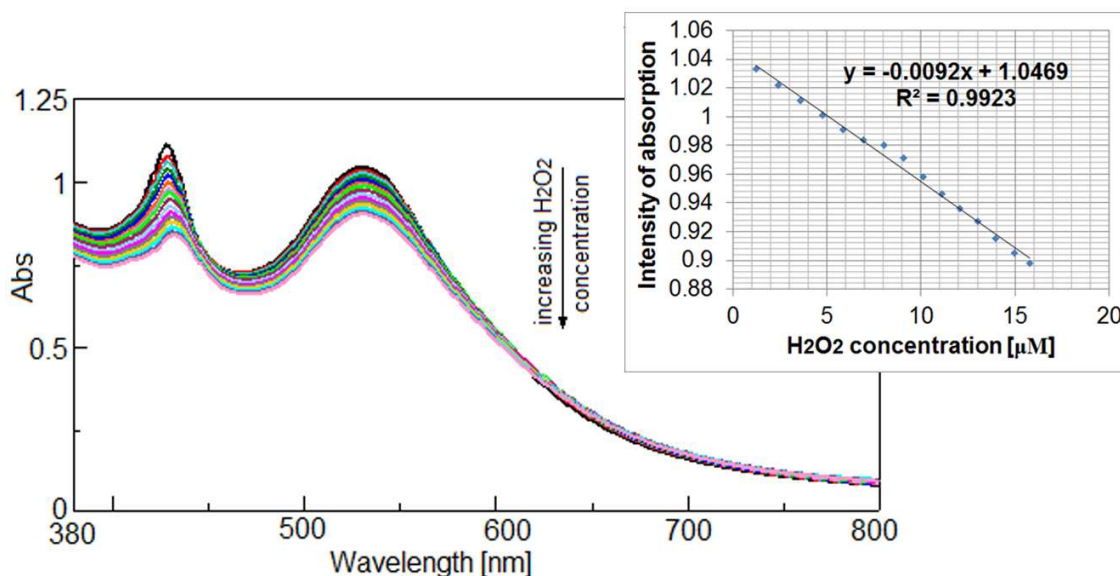


**Fig. 6.** Images obtained in STEM mode during the study of the interaction between **Co-3OHPP** and **nAu** deposited on TEM grids.

In order to test the capacity to detect  $\text{H}_2\text{O}_2$ , a mixture composed of 3 mL gold colloid solution ( $0.47 \times 10^{-3}$  M) and 1 mL **Co-3OHPP** ( $10^{-5}$  M) in THF solution (the mixture that provided **Co-3OHPP-nAu** complex with the highest intensity absorption in UV-vis analysis - see Fig. 4) was used. To this mixture portions of 50  $\mu\text{L}$   $\text{H}_2\text{O}_2$  solution (30 wt %) were successively added, stirred and UV-vis monitored (Fig. 7).

The absorption intensity of the gold-porphyrin complex is gradually decreasing with the increasing of  $\text{H}_2\text{O}_2$  concentration. There is a linear dependence between the concentration of

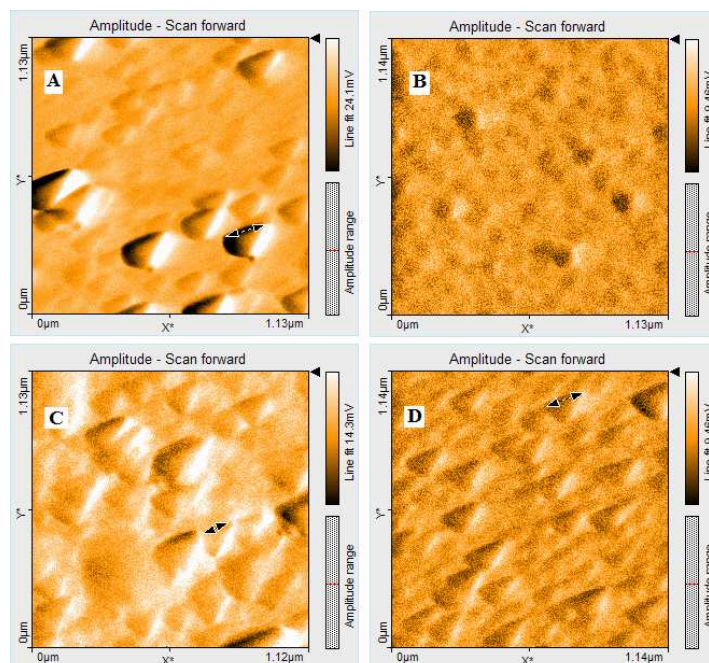
hydrogen peroxide and the intensity of absorption of the plasmonic complex, characterized by an excellent correlation coefficient of 0.992 (Fig. 7).



**Fig. 7.** UV-vis spectra after successive H<sub>2</sub>O<sub>2</sub> adding. Dependence between the concentration of hydrogen peroxide and the intensity of absorption of the plasmon.

AFM analysis showed that the behavior of the cobalt porphyrin is in accordance with our previous studies [17, 26] regarding the morphology and aggregation architectures of porphyrin derivatives from different solvents. The nanosized particles of **Co-3OHPP** are evenly oriented, have the shape of uniform triangular lamels and are displayed at different depths (Fig. 8A). The gold colloid as deposited on silica plate is associated in larger spherical aggregates (Fig. 8B). In case of the hybrid complex, the triangular shaped, well oriented porphyrin particles are embedded in the gold colloid matrix and the particle H-aggregation process into sandwich type geometry is more visible than in the case of cobalt porphyrin alone (Fig. 8C). After H<sub>2</sub>O<sub>2</sub> adding

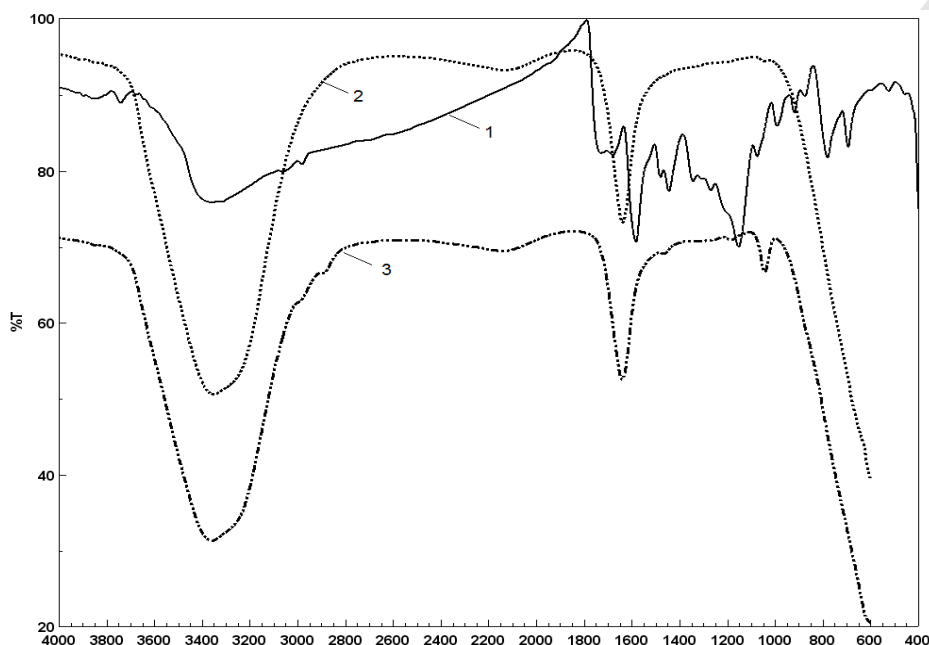
the whole material is completely restructured and the J- and H-aggregation processes are amplified creating a more uniform and compacted surface (Fig. 8D).



**Fig. 8.** AFM images in noncontact mode for Co-porphyrin (A), gold colloid (B), gold-porphyrin hybrid complex (C) and after  $\text{H}_2\text{O}_2$  treatment of the complex (D).

The changes in structure of the investigated materials were comparatively studied also by FT-IR spectroscopy. In the FT-IR spectrum of bare hybrid gold colloid-porphyrin and after  $\text{H}_2\text{O}_2$  exposure (Fig. 9, lines 2, 3) the large bands around  $3350\text{ cm}^{-1}$  and novel high intensity bands from  $1644\text{ cm}^{-1}$  can be attributed to the stretching mode and bending mode of  $\text{H}_2\text{O}$  molecules, respectively [27]. A number of low intensity IR bands are displayed both in bare Co II-porphyrin and in the hybrids of gold colloid-porphyrin in the region  $900\text{--}1050\text{ cm}^{-1}$ , due to in plane ring vibrations of porphyrin. The most important band, from around  $1650\text{ cm}^{-1}$ , that is differently shifted in FT-IR spectra to lower or higher wavenumbers, could be attributed to out-

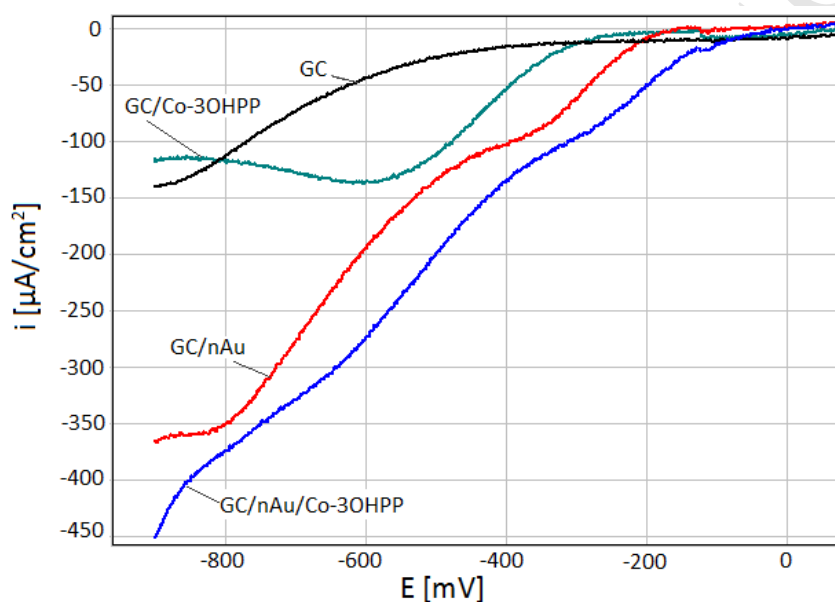
of-plane breathing of pyrrole rings, due to changes in the cobalt coordination after exposure to  $\text{H}_2\text{O}_2$  (Figure 9, line 2).



**Fig. 9.** Overlapped FT-IR spectra: **Co-3OHPP** (1); gold-porphyrin complex treated with  $\text{H}_2\text{O}_2$  (2); gold-porphyrin complex (3).

**Electrocatalysis of  $\text{H}_2\text{O}_2$  at  $n\text{Au}/\text{Co-3OHPP}$  composite film.** From the representations of linear voltammograms for all three modified **GC** electrodes in the presence of  $\text{H}_2\text{O}_2$  (Fig. 10) it can be observed that the process of reduction begins around:  $-100$  mV for **GC/nAu/Co-3OHPP**,  $-200$  mV for **GC/nAu** and  $-300$  mV for **GC/Co-3OHPP** respectively. Besides, the reduction currents for all three modified electrodes are higher than that of the **GC** electrode, that confirms the electrocatalytic character of the modified electrodes. The increase of the intensity of cathodic currents and the shift of the potential for the  $\text{H}_2\text{O}_2$  reduction current peak towards more

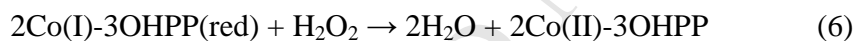
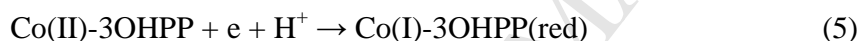
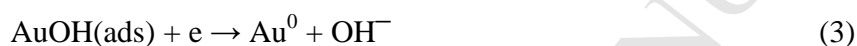
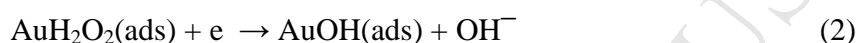
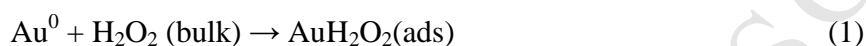
positive potentials might be caused by a synergic effect produced on one hand by **nAu**, that might increase the electrode active surface area and can favour a fast direct electron transfer from the layered Co-porphyrin and on the other hand, because of the favouring electron transfer effect of the Co-porphyrin activated electroactive centers (enhanced due to electron-donating properties of the hydroxyl groups). This type of behaviour was previously reported by other researchers regarding other types of substituted porphyrins or phtalocianines, such as: hemoglobin [28, 29], Co-diverse substituted porphyrins [30], cobalt tetracarboxylic acid phthalocyanine [31].



**Fig. 10.** Linear voltammograms showing the electrocatalytic reduction of hydrogen peroxide with bare **GC**; **GC** modified with **Co-3OHPP**, **nAu** and **nAu/Co-3OHPP**, in phosphate buffer electrolyte solution (pH 5.8) with  $1.16 \mu\text{M H}_2\text{O}_2$ .

The reaction mechanism for the reduction of  $\text{H}_2\text{O}_2$  to  $\text{H}_2\text{O}$  through the active centers of the Au nanoparticles and the electrocatalytic effect of the metalloporphyrin involving the  $\text{CoII}/\text{CoI}$  system is presented according with eqs. (1)-(8) and discussed by similitude with

reported electrocatalytic systems [31-33]. The mechanism presumes the adsorption of  $\text{H}_2\text{O}_2$  on the electrode surface followed by a two electron transfer in the presence of  $\text{H}^+$  ions and the formation of the final product,  $\text{H}_2\text{O}$ . These assumptions are also sustained by our experimental results. On the **GC/nAu** electrode (Fig 11) the supposed reaction steps are presented by the equations (1)- (4). The porphyrin layer from the electrode acts as an electron transfer mediator involving the redox couple  $\text{Co(II)/Co(I)}$  for the cathodic branch and the  $\text{Co(II)/Co(III)}$  system for the anodic reaction (Fig. 12), eqs. (5)-(8).



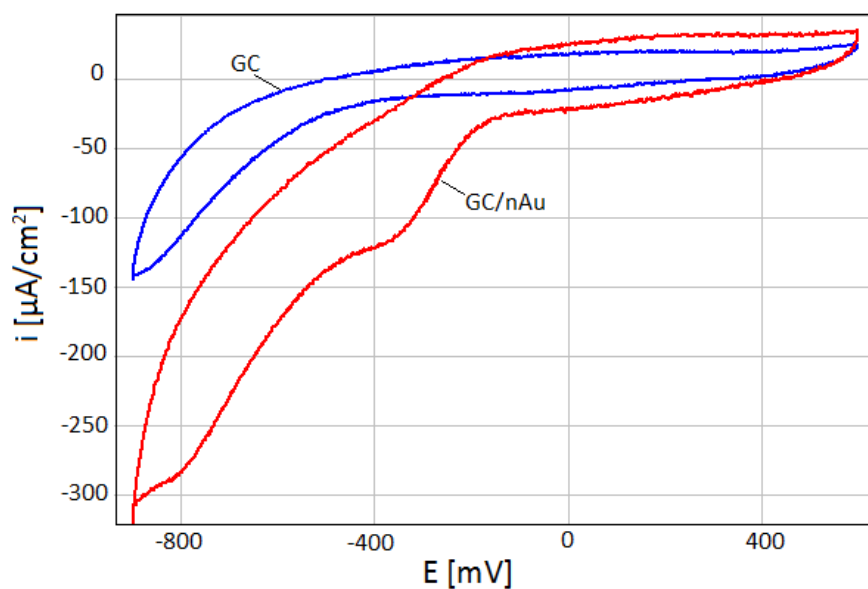


**Fig. 11.** Cyclic voltammograms of GC modified with nAu in 0.05M PBS solution and 0.58  $\mu\text{M}$   $\text{H}_2\text{O}_2$ .

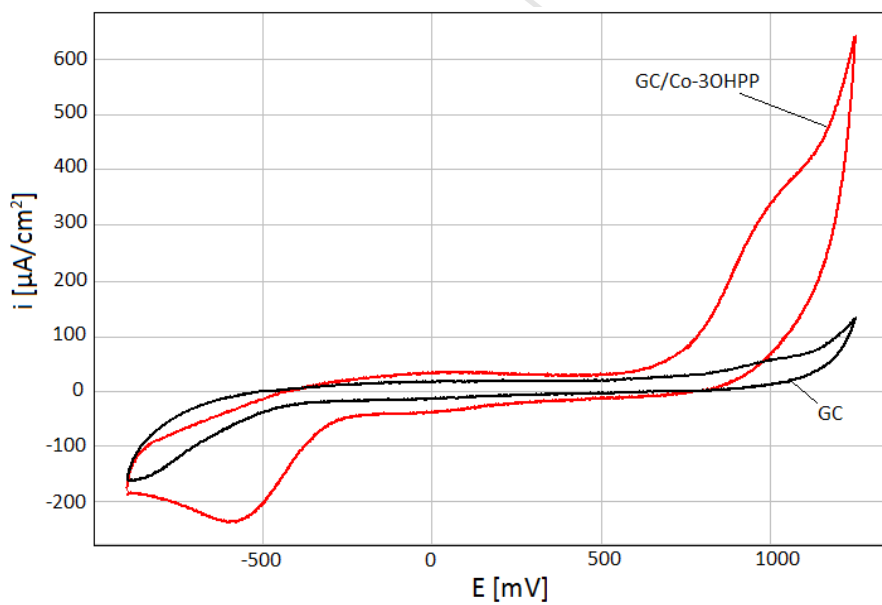


**Fig. 12.** Cyclic voltammograms of GC modified with Co-3OHPP in 0.05M PBS solution and 1.16  $\mu\text{M}$   $\text{H}_2\text{O}_2$ .

The influence of the  $\text{H}_2\text{O}_2$  concentration on the cathodic currents for the GC modified with **nAu/Co-3OHPP** is presented in Fig. 13, where the square-wave voltammetric response is given. The increase of the intensity of cathodic current can be noticed as the concentration of  $\text{H}_2\text{O}_2$  becomes higher (from  $17.6 \mu\text{M}$  up to  $1.7 \text{mM}$ ), these results offering the premises for further investigations of the possibility to use this electrode as sensor for hydrogen peroxide. The linear dependence between the  $\Delta i_c$  and the  $\text{H}_2\text{O}_2$  concentration is characterized by an excellent correlation coefficient.

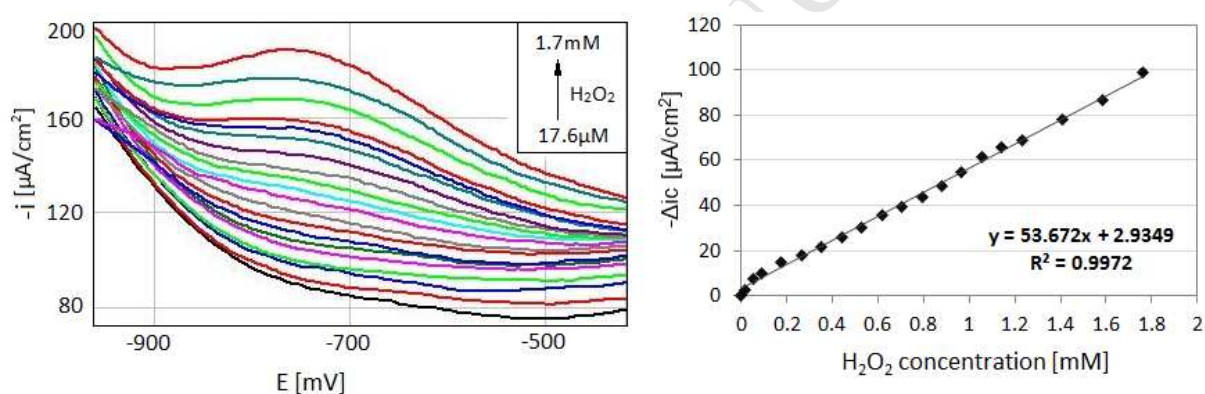


**Fig. 13.** The square-wave voltammetric response (SWV) of GC modified with **nAu/Co-3OHPP** films in the absence or presence of different concentrations of  $\text{H}_2\text{O}_2$ :  $0.017 \div 1.76 \text{mM}$ , in  $0.05 \text{M}$  PBS/ $0.05 \text{M}$  KCl solution. Dependence between cathodic current ( $\Delta i_c$ ) and  $\text{H}_2\text{O}_2$  concentration (at  $E = -750 \text{mV}$ ).

## Conclusions

Gold nanoparticles smaller than  $20 \text{nm}$  have been functionalized with Co(II) 5,10,15,20-meso-tetra(3-hydroxyphenyl) porphyrin (**Co-3OHPP**). The porphyrin-gold hybrid complex

showed wide band absorption in the UV-vis spectrum. The gold colloid proved its sensitivity to small amounts of porphyrin detection showing an excellent linear dependence between the intensity of absorption of the gold plasmonic band and the increasing concentration in **Co-3OHPP**. This result might find valuable medical applications because abnormal levels of porphyrin derivatives (porphobilinogen, aminolevulinic acid, uroporphyrin, coproporphyrin, protoporphyrin) present in human body are indicative for many metabolic diseases (diabetes, porphyria, kidney diseases).

The **nAu**-porphyrin complex was exposed to increased amounts of  $\text{H}_2\text{O}_2$  and the changes of the absorption spectra were monitored by UV-vis spectroscopy, proving its sensing capacity. The absorption intensity of the gold-porphyrin complex is gradually decreasing with the increasing of  $\text{H}_2\text{O}_2$  concentration. The process is reproducible and there is a linear dependence between the concentration of hydrogen peroxide and the intensity of absorption of the plasmonic complex. The same experiment performed on bare gold colloidal solution led to chaotic response of the plasmon intensity function of  $\text{H}_2\text{O}_2$  concentration, proving that the presence of metalloporphyrin is indispensable for detection.

The FT-IR and AFM studies showed significant structural and morphological modifications of the hybrid material after  $\text{H}_2\text{O}_2$  exposure. The AFM investigations show the morphological changes that take place for each procedure. Thus, in case of the complex formation between **Co-3OHPP** and gold nanoparticles, porphyrin particles are embedded in the gold colloid matrix and the particle H-aggregation process is more visible than in the case of cobalt porphyrin alone. STEM investigation of the complex between **Co-3OHPP** and gold nanoparticles revealed some dendritic structures comprised mainly of **Co-3OHPP** H- and J-type self-aggregates due to their interaction with gold nanoparticles.

After  $\text{H}_2\text{O}_2$  adding the whole material is completely restructured and the J- and H-aggregation processes are amplified creating a more uniform and compacted surface. The FT-IR structure investigation shows that the Co coordination sphere changes after the exposure of the hybrid material to  $\text{H}_2\text{O}_2$ .

In order to enlarge the possibility of electroanalytical application of the **nAu/ Co-3OHPP** complex, modified glassy carbon electrodes were realized by deposition of **nAu** and **Co-3OHPP** alone and of ordered layers **nAu-Co-3OHPP** and were comparatively tested by linear and cyclic voltammetry to evidence their response to  $\text{H}_2\text{O}_2$ . The electrocatalytic effect of the **nAu/ Co-3OHPP** hybrid system for the electrochemical reduction of hydrogen peroxide in the range of physiologically-relevant levels creates the opportunity to use modified **GC** electrodes with ordered layers for  $\text{H}_2\text{O}_2$  analyses.

The further incorporation of **nAu/Co-3OHPP** hybrid material into miniaturized electrochemical detecting devices is our future goal. Other promising applications of this material could be in medicine, where the transport of porphyrins into cells by means of nontoxic gold nanoparticles is of great interest for imaging [34] and PDT of cancer diseases [35] and in formulation of photovoltaic cells [36].

**Acknowledgements:** The authors from Institute of Chemistry Timisoara of Romanian Academy are kindly acknowledging the support from Program 3-Porphyrins/2015 and STAR Programme- SAFEAIR Project 76/2013. This work is dedicated to Anniversary of 150 years since the establishment of Romanian Academy.

## References

- [1] M. Pędziwiatr, R. Wiglusz, A. Graczyk, J. Legendziewicz, Photophysics of the porphyrins and hybrid materials obtained on their basis: A prospective chiral biosensor, *J. Alloys Compd.* 451 (2008) 46-51.
- [2] X. Su, J. Li, Z. Zhang, M. Yu, L. Yuan, Cu(II) porphyrins modified TiO<sub>2</sub> photocatalysts: Accumulated patterns of Cu(II) porphyrin molecules on the surface of TiO<sub>2</sub> and influence on photocatalytic activity, *J Alloys Compd.* 626, (2015) 252-259.
- [3] M. Goswami, V. Lyaskovskyy, S. R. Domingos, W. J. Buma, S. Woutersen, O. Troeppner, I. Ivanović-Burmazović, H. Lu, X. Cui, X. P. Zhang, E. J. Reijerse, S. DeBeer, M. M. van Schooneveld, F. F. Pfaff, K. Ray, B. de Bruin, Characterization of Porphyrin-Co(III)-'Nitrene Radical' Species Relevant in Catalytic Nitrene Transfer Reactions, *J. Am. Chem. Soc.* 137 (2015) 5468-5479.
- [4] M. A. Morales Vásquez, S. A. Suárez, F. Doctorovich, Gold and silver anchored cobalt porphyrins used for catalytic water splitting, *Materials Chemistry and Physics*, 2015, p. 159-166.
- [5] W. Ma, P. Yu, T. Ohsaka, L. Mao, An efficient electrocatalyst for oxygen reduction reaction derived from a Co-porphyrin-based covalent organic framework, *Electrochem. Commun.* 52 (2015) 53-57.
- [6] J. F. Cabrita, A. S. Viana, F.-P. Montforts, L. M. Abrantes, Mixed self-assembled monolayers of Co-porphyrin and n-alkane phosphonates on gold, *Surf. Sci.* 605 (2011) 1412-1419.
- [7] C. S. Eberle, A. S. Viana, F.-P. Montforts, L. M. Abrantes, Synthesis and self-assembly of a novel cobalt(II) porphyrin lipoic acid derivative on gold, *J. Porphyr. Phthalocyanines*, 14 (2010) 101-107.

- [8] W. Zhang, A.U. Shaikh, E.Y. Tsui, T.M. Swager, Cobalt Porphyrin Functionalized Carbon Nanotubes for Oxygen Reduction, *Chem. Mater.* 21 (2009) 3234-3241.
- [9] S. Zoladek, I. A. Rutkowska, M. Blicharska, K. Skorupska, P. J. Kulesza, Enhancement of oxygen reduction at Co-porphyrin catalyst by supporting onto hybrid multi-layered film of polypyrrole and polyoxometalate-modified gold nanoparticles, *J. Solid State Electr.* 20 (2016) 1199-1208.
- [10] Y. Shen, F. Zhan, J. Lu, B. Zhang, D. Huang, X. Xu, Y. Zhang, M. Wan, Preparation of hybrid films containing gold nanoparticles and cobalt porphyrin with flexible electrochemical properties, *Thin Solid Films* 545 (2013) 327–331.
- [11] H. Kim, Y. H. Chang, S.-H. Lee, Y.-H. Kim, S.-J. Kahng, Switching and Sensing Spin States of Co–Porphyrin in Bimolecular Reactions on Au(111) Using Scanning Tunneling Microscopy, *ACS Nano* 7 (2013) 9312-9317.
- [12] Y. Kalachyova, O. Lyutakov, A. Solovyev, P. Slepíčka, V. Švorčík, Surface morphology and optical properties of porphyrin/Au and Au/porphyrin/Au systems, *Nanoscale Res. Lett.* 8 (2013) 547 doi: 10.1186/1556-276X-8-547.
- [13] J. Shu, Z. Qiu, Q. Wei, J. Zhuang, D. Tang, Cobalt-Porphyrin-Platinum-Functionalized Reduced Graphene Oxide Hybrid Nanostructures: A Novel Peroxidase Mimetic System For Improved Electrochemical Immunoassay, *Scientific Reports* 5: 15113 (2015), doi:10.1038/srep15113.
- [14] L. Feng, L. Tianjun, W. Li, Synthesis, Characterization and Cell-uptake of Porphyrin-capped Gold Nanoparticle, Chapter 7th Asian-Pacific Conference on Medical and Biological Engineering, Volume 19 of the series IFMBE Proceedings 2008, Eds. Y. Peng, X. Weng, Springer Verlag, Berlin, p. 186-189.

- [15] L.A. Dykman, N.G. Khlebtsov, Gold Nanoparticles in Biology and Medicine: Recent Advances and Prospects, *Acta Naturae* 2 (2011) 34-55.
- [16] M.-C. Daniel, D. Astruc, Gold Nanoparticles: Assembly, Supramolecular Chemistry, Quantum-Size-Related Properties, and Applications toward Biology, Catalysis and Nanotechnology, *Chem. Rev.* 104 (2004) 293-346.
- [17] A. Lascu, A. Palade, G. Fagadar-Cosma, I. Creanga, C. Ianasi, I. Sebarchievici, M. Birdeanu, E. Fagadar-Cosma, Mesoporous manganese–porphyrin–silica hybrid nanomaterial sensitive to H<sub>2</sub>O<sub>2</sub> fluorescent detection, *Mater. Res. Bull.* 74 (2016) 325-332.
- [18] E. Fagadar-Cosma, E. Tarabukina, N. Zakharova, M. Birdeanu, B. Taranu, A. Palade, I. Creanga, A. Lascu, G. Fagadar-Cosma, Hybrids formed between polyvinylpyrrolidone and an A<sub>3</sub>B porphyrin dye: behavior in aqueous solutions and chemical response to CO<sub>2</sub> presence, *Polym. Int.* 65 (2015) 200-209.
- [19] X. Huang, M. A. El-Sayed, Gold nanoparticles: Optical properties and implementations in cancer diagnosis and photothermal therapy, *J. Adv. Res.* 1 (2010) 13-28.
- [20] C. Cretu, C. Bucovicean, I. Armeanu, A.M. Lacrama, E. Fagadar-Cosma, Synthesis and spectroscopic characterization of meso-tetra (3-hydroxyphenyl) porphyrin, Synthesis and spectroscopic characterization of meso-tetra (3-hydroxyphenyl) porphyrin, *Rev. Chim.* 59 (2008) 979-981.
- [21] E. Fagadar-Cosma, M. Mirica, I. Balcu, C. Bucovicean, C. Cretu, I. Armeanu, G. Fagadar-Cosma, Syntheses, Spectroscopic and AFM Characterization of Some Manganese Porphyrins and Their Hybrid Silica Nanomaterials., *Molecules* 14 (2009) 1370-1388.

- [22] P. Muthukumar, S. Abraham John, Gold nanoparticles decorated on cobalt porphyrin-modified glassy carbon electrode for the sensitive determination of nitrite ion, *J. Colloid Interf. Sci.* 421 (2014) 78-84.
- [23] Y.L. Chen, Y.C. Huang, C.C. Wang, Direct assay of uroporphyrin and coproporphyrin in human urine by reverse-mode field amplified sample injection-sweeping and micellar electrokinetic chromatography, *Talanta* 143 (2015) 27-34.
- [24] E. Fagadar-Cosma, Z. Dudás, M. Birdeanu, L. Almásy, Hybrid organic – silica nanomaterials based on novel A<sub>3</sub>B mixed substituted porphyrin, *Mat. Chem. Phys.* 148 (2014) 143-152.
- [25] B. O. Taranu, I. Sebarchievici, I. Taranu, M. Birdeanu, E. Fagadar- Cosma, Electrochemical and Microscopic Characterization of Two meso-Substituted A<sub>3</sub>B and A<sub>4</sub> Porphyrins, *Rev.Chim.(Bucharest)*, 67 (2016) 892-896.
- [26] E. Fagadar-Cosma, D. Vlascici, G. Fagadar-Cosma, A. Palade, A. Lascu, I. Creanga, M. Birdeanu, R. Cristescu, I. Cernica, A Sensitive A<sub>3</sub>B Porphyrin Nanomaterial for CO<sub>2</sub> Detection, *Molecules* 19 (2014) 21239-21252.
- [27] P. Şen, C. Hirel, C. Andraud, C. Aronica, Y. Bretonnière, A. Mohammed, H. Ågren, B. Minaev, V. Minaeva, G. Baryshnikov, H.-H. Lee, J. Duboisset, M. Lindgren, Fluorescence and FTIR Spectra Analysis of Trans-A<sub>2</sub>B<sub>2</sub>- Substituted Di- and Tetra-Phenyl Porphyrins, *Materials* 3 (2010) 4446-4475.
- [28] J. Hong, Y.X. Zhao, B.L. Xiao, A.A. Moosavi-Movahedi, H. Ghourchian, N. Sheibani, Direct electrochemistry of hemoglobin immobilized on a functionalized multi-walled carbon nanotubes and gold nanoparticles nanocomplex-modified glassy carbon electrode, *Sensors* 13 (2013) 8595-8611.

- [29] Y. Liu, Q.Y. Jiang, S.Y. Lu, Y. Zhang, H.Y. Gu, Immobilization of hemoglobin on the gold colloid modified pretreated glassy carbon electrode for preparing a novel hydrogen peroxide biosensor, *Appl. Biochem. Biotechnol.* 152 (2009) 418–427.
- [30] M. Yuasa, B. Steiger, F.C. Anson, Hydroxy-substituted cobalt tetraphenylporphyrins as electrocatalysts for the reduction of O<sub>2</sub>, *J. Porphyr. Phthalocyanines* 1 (1997) 181–188.
- [31] P.N. Mashazi, K.I. Ozoemena, T. Nyokong, Tetracarboxylic acid cobalt phthalocyanine SAM on gold: Potential applications as amperometric sensor for H<sub>2</sub>O<sub>2</sub> and fabrication of glucose biosensor, *Electrochimica Acta* 52 (2006) 177–186.
- [32] K.S. Lokesh, A. Shambhulinga, N. Manjunatha, M. Imadadulla, M. Hojamberdiev, Porphyrin macrocycle-stabilized gold and silver nanoparticles and their application in catalysis of hydrogen peroxide, *Dyes Pigm.* 120 (2015) 155-160.
- [33] S. Patra, N. Munichandraiah, Electrochemical reduction of hydrogen peroxide on stainless steel, *J. Chem. Sci.* 121 (2009) 675–683.
- [34] N. Kemikli, H. Kavas, S. Kazan, A. Baykal, R. Ozturk, Synthesis of protoporphyrin coated superparamagnetic iron oxide nanoparticles via dopamine anchor, *J. Alloys Compd.* 502 (2010) 439-444.
- [35] M. Ethirajan, Y. Chen, P. Joshi, R.K. Pandey, The role of porphyrin chemistry in tumor imaging and photodynamic therapy, *Chem. Soc. Rev.* 40 (2011) 340-62.
- [36] G. Mihailescu, L. Olenic, S. Garabagiu, G. Blanita, E. Fagadar-Cosma, A.S.Biris, Coupling Between Plasmonic Resonances in Nanoparticles and Porphyrins Molecules, *J. Nanosci. Nanotech.* 10 (2010) 2527-2530.

**Highlights**

- ▶ Wide UV-vis absorption band gold-metalloporphyrin hybrid was obtained.
- ▶ Gold nanoparticles are sensitive to trace amounts of Co-porphyrin.
- ▶ Gold-Co-porphyrin complex is sensitive to H<sub>2</sub>O<sub>2</sub> detection by UV-vis spectroscopy.
- ▶ Co-porphyrin/gold nanoparticle-modified glassy carbon electrodes were tested.
- ▶ Modified electrodes show electrocatalytic effect on the reduction of H<sub>2</sub>O<sub>2</sub>.